

# COSMOLOGICAL PARAMETERS FROM THE CLUSTERING OF AGN

Spyros Basilakos

*Astrophysics Group, Imperial College London, Blackett Laboratory,*

*Prince Consort Road, London SW7 2BW, UK*

s.basilakos@ic.ac.uk

## Abstract

We attempt to put constraints on different cosmological and biasing models by combining the recent clustering results of X-ray sources in the local ( $z \leq 0.1$ ) and distant universe ( $z \sim 1$ ). To this end we compare the measured angular correlation function for bright [1] and faint [20] *ROSAT* X-ray sources respectively with those expected in three spatially flat cosmological models. Taking into account the different functional forms of the bias evolution, we find that there are two cosmological models which match well the data. In particular, low- $\Omega_0$  cosmological models ( $\Omega_\Lambda = 0.7$ ) that contain either (i) high  $\sigma_8^{\text{mass}} = 1.13$  or (ii) low  $\sigma_8^{\text{mass}} = 0.9$  respectively with different bias behaviour, best reproduce the AGN clustering results. While  $\tau$ CDM models with different bias behaviour are ruled out at a high significance level.

**Keywords:** galaxies: clustering- X-ray sources - cosmology:theory - large-scale structure of universe

## Introduction

The study of the distribution of matter on large scales, based on different extragalactic objects, provides important constraints on models of cosmic structure formation. In particular Active Galactic Nuclei (AGN) can be detected up to very high redshifts and therefore provide information on how the X-ray selected sources trace the underlying mass distribution as well as the evolution of large scale structure.

However, a serious problem here is how the luminous matter traces the underlying mass distribution. Many authors have claimed that the large scale clustering pattern of different mass tracers (galaxies or clusters) is characterized by a bias picture [8]. In this framework, biasing is

assumed to be statistical in nature; galaxies and clusters are identified as high peaks of an underlying, initially Gaussian, random density field. Biasing of galaxies with respect to the dark matter distribution was also found to be an essential ingredient of CDM models of galaxy formation in order to reproduce the observed galaxy distribution. Furthermore, different studies have shown that the bias factor,  $b(z)$ , is a monotonically increasing function of redshift [19]. For example, Steidel et al. [17] confirmed that the Lyman-break galaxies are very strongly biased tracers of mass and they found that  $b(z = 3.4) \simeq 6, 4, 2$ , for SCDM,  $\Lambda$ CDM ( $\Omega_o = 0.3$ ) and OCDM ( $\Omega_o = 0.2$ ), respectively.

Studies based on the traditional indicators of clustering, like the two point correlation function, have been utilized in order to describe the AGN clustering properties. Our knowledge regarding the AGN clustering comes mostly from optical surveys for QSO's ([16] and reference therein). It has been established, that QSO's have a clustering length of  $r_o \simeq 5.4 \pm 1.1h^{-1}\text{Mpc}$ .

Vikhlinin & Forman [20] studied the angular clustering properties using a set of deep *ROSAT* observations. Carrera et al. [5] combined two soft X-ray surveys (235 AGN), found a spatial correlation length  $1.5h^{-1}\text{Mpc} \leq r_o \leq 5.5h^{-1}\text{Mpc}$ , depending on the adopted model of clustering evolution. Recently, Akylas et al. [1] using 2096 sources detected in the *ROSAT* All Sky Survey Bright Source Catalogue (RASSBSC), derived the AGN angular correlation function in the nearby Universe and utilizing Limber's equation obtained  $r_o = 6.7 \pm 1.0h^{-1}\text{Mpc}$ , assuming comoving clustering evolution.

Here, we present the standard theoretical approach to estimate the angular correlation function  $w(\theta)$ , using different models for the bias evolution in different spatially flat cosmological models. Comparing the latter with observational results, we attempt to put constraints on the different cosmological and bias models

## 1. The Integral Equation of Clustering

For the purpose of this study we utilize the relation between the angular  $w(\theta)$  and spatial  $\xi(r, z)$  two point correlation functions ([10] and references therein). As it is well known, this connection can be done using the Limber equation [14]. For example, in the case of a spatially flat Universe ( $\Omega_o + \Omega_\Lambda = 1$ ), the Limber equation can be written as

$$w(\theta) = 2 \frac{H_o}{c} \frac{\int_0^\infty N^2(z) E(z) dz \int_0^\infty \xi(r, z) du}{[\int_0^\infty N(z) dz]^2} . \quad (1)$$

where  $x$  is the comoving coordinate related to the redshift through

$$x = \frac{c}{H_0} \int_0^z \frac{dy}{E(y)} , \quad (2)$$

with

$$E(z) = [\Omega_o(1+z)^3 + \Omega_\Lambda]^{1/2} \quad (3)$$

[14]. The mean surface density,  $\mathcal{N}$ , on a survey of solid angle  $\Omega_s$  is:

$$\mathcal{N} = \int_0^\infty x^2 \phi(x) dx = \frac{1}{\Omega_s} \int_0^\infty N(z) dz , \quad (4)$$

where  $N(z)$  is the number of objects in the given survey within the shell  $(z, z + dz)$  and  $\phi(x)$  is the selection function (the probability that a source at a distance  $x$  is detected in the survey):

$$\phi(x) = \int_{L_{\min}}^\infty \Phi(L_x, z) dL . \quad (5)$$

In this work we used a luminosity function  $\Phi(L_x, z)$  of the form assumed by Boyle et al. [4].

The physical separation between two sources, separated by an angle  $\theta$  considering a small angle approximation is given by:

$$r \simeq \frac{1}{(1+z)} (u^2 + x^2 \theta^2)^2 . \quad (6)$$

Extending this picture, we quantify the evolution of clustering with epoch presenting the spatial correlation function of the X-ray sources as

$$\xi(r, z) = \xi_{\text{mass}}(r) R(z) , \quad (7)$$

with  $R(z) = D^2(z)b^2(z)$ , where  $D(z)$  is the linear growth rate of clustering (cf. Peebles 1993) being given by

$$D(z) = \frac{5\Omega_o E(z)}{2} \int_z^\infty \frac{(1+y)}{E^3(y)} dy \quad (8)$$

and finally  $b(z)$  is the evolution of bias.

## 2. Bias Evolution

The concept of biasing between different classes of extragalactic objects and the background matter distribution was put forward by Kaiser [8] in order to explain the higher amplitude of the 2-point correlation function of clusters of galaxies with respect to that of galaxies themselves. Therefore, we shortly describe here some of the bias evolution models in order to introduce them to our analysis.

### 2.1. No evolution of bias (B0)

This model considers constant bias at all epochs:

$$b(z) = b_o \simeq b_o^{\text{opt}} \left( \frac{r_o}{r_o^{\text{opt}}} \right)^{\gamma/2} \quad (9)$$

where  $r_o^{\text{opt}} = 5.4h^{-1}\text{Mpc}$  is the correlation length in comoving coordinates estimated by the APM correlation function [9] and  $r_o$  is the corresponding length for the X-ray sources. Finally,  $b_o^{\text{opt}} = 1/\sigma_8^{\text{mass}}$  is the present bias of optical galaxies relative to the distribution of mass and  $\sigma_8^{\text{mass}}$  is the mass rms fluctuations in sphere of radius  $8h^{-1}\text{Mpc}$ . Using the above ideas, if one assumes that  $r_o > r_o^{\text{opt}}$ , then it is quite obvious that the X-ray sources are indeed more biased with respect to optical galaxies by the factor  $(r_o/r_o^{\text{opt}})^{\gamma/2}$ . In case that  $b(z) \equiv 1$ , we have the so called non-bias model (from now on we consider  $b(z) \equiv 1$  as a (B0) bias model).

### 2.2. Test Particle or Galaxy Conserving Bias (B1)

This model, proposed by many authors ([19] and references therein), predicts the evolution of bias, independent of the mass and the origin of halos, assuming only that the test particles fluctuation field is related proportionally to that of the underlying mass. Thus, the bias factor as a function of redshift can be written:

$$b(z) = 1 + \frac{(b_o - 1)}{D(z)} \quad , \quad (10)$$

where  $b_o$  is the bias factor at the present time.

### 2.3. Merging Bias Model (B2)

Mo & White [13] have developed a model for the evolution of the correlation bias, using the Press-Schechter formalism. Utilizing a similar formalism, Matarrese et al. [12] extended the Mo & White results to include the effects of different mass scales. In this case we have that

$$b(z) = 0.41 + \frac{(b_o - 0.41)}{D(z)^{1.8}} \quad . \quad (11)$$

## 3. Cold Dark Matter (CDM) Cosmologies

In this section, we present the cosmological models that we use in this work. For the power spectrum of our CDM models, we consider  $P(k) \approx$

$k^n T^2(k)$  with scale-invariant ( $n = 1$ ) primeval inflationary fluctuations. We utilize the transfer function parameterization as in Bardeen et al. [2], with the corrections given approximately by Sugiyama's [18] formula:

$$T(k) = \frac{\ln(1 + 2.34q)}{2.34q} [1 + 3.89q + (16.1q)^2 + (5.46q)^3 + (6.71q)^4]^{-1/4} .$$

with  $q = k/h\Gamma$ , where  $k = 2\pi/\lambda$  is the wavenumber in units of  $h \text{ Mpc}^{-1}$  and  $\Gamma$  is the CDM shape parameter in units of  $(h^{-1}\text{Mpc})^{-1}$ . In this analysis, we have taken into account three different cold dark matter models (CDM) in order to isolate the effects of different parameters on the X-ray sources clustering predictions.

The  $\tau$ CDM ( $\Omega_o = 1$ ,  $h = 0.5$ ,  $\sigma_8^{\text{mass}} = 0.55$ ,  $b_o = 2.18$ ) and  $\Lambda$ CDM ( $\Omega_\Lambda = 0.7$ ,  $h = 0.65$ ,  $\sigma_8^{\text{mass}} = 0.9$ ,  $b_o = 1.33$ ) [11] are approximately COBE normalized and the latter cosmological model is consistent with the results from Type Ia supernova [15]. In the same framework, the  $\tau$ CDM and  $\Lambda$ CDM models have  $\Gamma \sim 0.2$ , in approximate agreement with the shape parameter estimated from galaxy surveys [9] and they have fluctuation amplitude in  $8 h^{-1}\text{Mpc}$  scale,  $\sigma_8^{\text{mass}}$ , consistent with the cluster abundance,  $\sigma_8^{\text{mass}} = 0.55\Omega_o^{-0.6}$  [7].

Furthermore, in order to investigate cosmological models with high value of  $\sigma_8^{\text{mass}}$ , we include a new model named  $\Lambda$ CDM2 ( $\Omega_\Lambda = 0.7$ ,  $h = 0.6$ ,  $\sigma_8^{\text{mass}} = 1.13$ ,  $b_o = 1.06$ ) [6]. The  $\sigma_8^{\text{mass}}$  value for the latter cosmological model is in good agreement with both cluster and the 4-years COBE data with a shape parameter  $\Gamma = 0.25$ . Therefore, it is quite obvious that two of our models ( $\tau$ CDM and  $\Lambda$ CDM) have the same power spectrum and geometry but different values of  $\Omega_o$  and  $\sigma_8^{\text{mass}}$ , while the two spatially flat, low-density CDM models ( $\Lambda$ CDM and  $\Lambda$ CDM2) have different  $\sigma_8$  and  $\Gamma$  respectively. It turns out that in  $\Lambda$ CDM and  $\tau$ CDM models the distribution of X-ray sources is "biased" relative to the distribution of mass; while the  $\Lambda$ CDM2 model is almost non "biased" while  $b_o$  at the present time is described by equation (9).

In order to understand better the effects of AGN clustering, we present in figure 1 the quantity  $R(z) = D^2(z)b^2(z)$  as a function of redshift for the three cosmological models, utilizing at the same time different bias evolution. It is quite obvious that the behaviour of the function  $R(z)$  characterizes the clustering evolution with epoch. Figure 1, for example, clearly shows that the bias at high redshifts has different values in different cosmological models. In particular for the high  $\sigma_8^{\text{mass}}$  low- $\Omega_o$  flat model ( $\Lambda$ CDM2) the distribution of X-ray sources is only weakly biased, as opposed to the strongly biased distribution in the  $\tau$ CDM cosmological model.

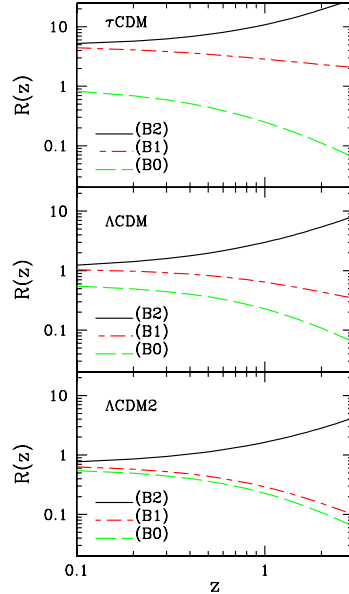
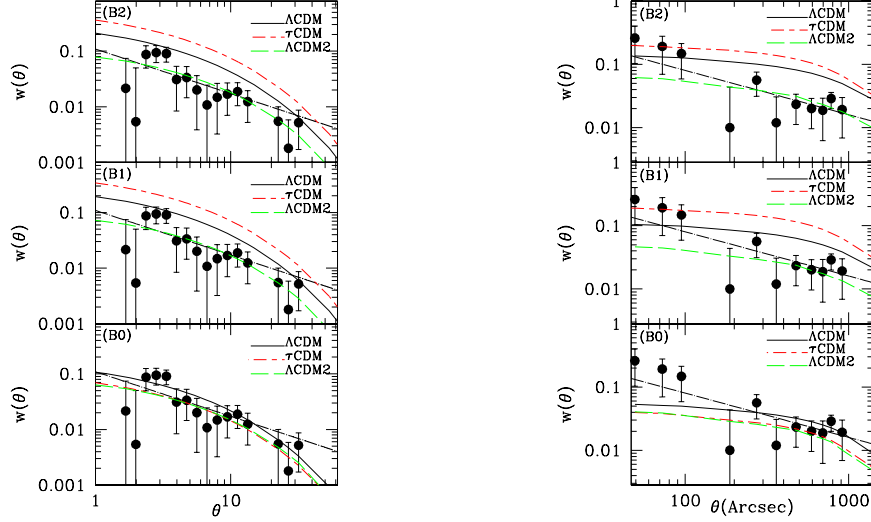


Figure 1. The function  $R(z)$  as a function of  $z$ , for different bias evolution models.

Indeed the different functional forms of  $b(z)$ , provide clustering models where: (i) AGN clustering is a decreasing function with redshift for (B0), (ii) AGN clustering is roughly constant for (B1). However, the  $\Lambda$ CDM2-B1 model gives lower  $R(z)$  simply because the higher  $\sigma_8^{\text{mass}}$  normalization largely removes the clustering difference between the two other flat cosmological models with low  $\sigma_8^{\text{mass}}$  normalizations. In other words, the present bias value of the above model is almost  $\sim 1$ , which gives clustering behaviour similar to the  $\Lambda$ CDM2-B0. Finally, AGN clustering is a monotonically increasing function of redshift for (B2) and (B3) respectively ([3] for details).

#### 4. Application to the Data

In Figure 2 (left) we compare the angular correlation function of a sample of 2096 sources with a total sky coverage of 4.9sr detected in the *ROSAT* All-Sky Survey Bright Source Catalogue [1] with that predicted in various flat cosmological models. Considering a two point angular correlation function of the form  $w(\theta) = (\theta/\theta_o)^{1-\gamma}$ , the above authors found  $\theta_o = 0.062^\circ$ ,  $\gamma = 1.8$  and spatial correlation length of  $r_o \approx 6.5 \pm 1.0h^{-1}\text{Mpc}$  and  $r_o \approx 6.7 \pm 1.0h^{-1}\text{Mpc}$  for stable and comoving clustering evolution respectively, similar to the optically selected AGN. Due to the fact that the above estimates have been focused on the local X-



*Figure 2.* Left: Comparison of the predicted angular correlation function for various cosmological models with that of the local AGN distribution, estimated in [1]. Errorbars are determined by assuming Poisson statistics. The continuous dot-dash line represent the best fit to  $w_x(\theta)$  derived by the above authors. Right: Comparison of the predicted angular correlation function for various models with that estimated in [20]. The continuous dot-dash line represent the best fit to  $w_x(\theta)$  derived by the above authors.

ray Universe, in this work we use complementary observational results from [20]. They have analysed a set of deep *ROSAT* observations with a total sky coverage of  $40 \text{ deg}^2$ , in order to investigate the clustering properties of faint X-ray sources. Therefore, they claimed that the two point angular correlation function is well described by a power law with  $\gamma = 1.8$ . Thus, in Figure 2 (right) we plot their results and the estimated angular correlation function for all nine models.

In order to quantify the differences between models and data, we perform a standard  $\chi^2$  test, for the bright (RASSBSC) and faint sources respectively, and we present the  $\mathcal{P}_{>\chi^2}^N$  (see table 2), where we have been use  $N = B, F$  for bright (RASSBSC) and faint X-ray sources respectively. Comparing the statistical results for both (a) high (faint sources) and (b) low (bright) redshift regimes, we can point out that for the bright X-ray sources the only models that are excluded by the data, at a relatively high significance level, are  $\Lambda\text{CDM-B2}$ ,  $\tau\text{CDM-B1}$  and  $\tau\text{CDM-B2}$ . Interestingly, for the faint objects the excluded models are  $\Lambda\text{CDM-B1}$ ,  $\Lambda\text{CDM-B2}$ ,  $\Lambda\text{CDM2-B0}$ ,  $\Lambda\text{CDM2-B1}$ ,  $\tau\text{CDM-B0}$ ,  $\tau\text{CDM-B1}$  and  $\tau\text{CDM-B2}$ . The above differences between the two kind of popula-

Table 1.  $\chi^2$  probabilities ( $\mathcal{P}_{>\chi^2}^{B,F}$ ) of consistency between RASSBSC, faint *ROSAT* data and models.

Comparison Pair	$\mathcal{P}_{>\chi^2}^B$	Comparison Pair	$\mathcal{P}_{>\chi^2}^F$
RASSBSC - $\Lambda$ CDM-B0	0.81	faint <i>ROSAT</i> - $\Lambda$ CDM-B0	0.037
RASSBSC - $\Lambda$ CDM-B1	0.067	faint <i>ROSAT</i> - $\Lambda$ CDM-B1	$3.67 \times 10^{-4}$
RASSBSC - $\Lambda$ CDM-B2	0.019	faint <i>ROSAT</i> - $\Lambda$ CDM-B2	$1.72 \times 10^{-6}$
RASSBSC - $\Lambda$ CDM2-B0	0.19	faint <i>ROSAT</i> - $\Lambda$ CDM2-B0	$3.44 \times 10^{-4}$
RASSBSC - $\Lambda$ CDM2-B1	0.42	faint <i>ROSAT</i> - $\Lambda$ CDM2-B1	$3.21 \times 10^{-3}$
RASSBSC - $\Lambda$ CDM2-B2	0.57	faint <i>ROSAT</i> - $\Lambda$ CDM2-B2	0.036
RASSBSC - $\tau$ CDM-B0	0.19	faint <i>ROSAT</i> - $\tau$ CDM-B0	$4.64 \times 10^{-3}$
RASSBSC - $\tau$ CDM-B1	$2.88 \times 10^{-8}$	faint <i>ROSAT</i> - $\tau$ CDM-B1	$1.07 \times 10^{-12}$
RASSBSC - $\tau$ CDM-B2	$3.00 \times 10^{-9}$	faint <i>ROSAT</i> - $\tau$ CDM-B2	$4.73 \times 10^{-15}$

tions are to be expected simply because the cosmological evolution plays an important role on large scale structure clustering due to the fact that the high redshift objects are more biased tracers of the underlying matter distribution with respect to the low redshift objects [17]. Also, from the faint X-ray sources results we would like to point out that there is not a single  $\tau$ CDM model that fits the data.

If we make the reasonable assumption that there is no correlation between the two X-ray populations, mostly due to the large distances involved, we can consider the RASSBSC and faint *ROSAT* catalogues as being independent of each other. Under this assumption the previous statistical tests can be considered as independent (as indeed verified by a KS test). Therefore, the joint (overall) probability can be given by the following expression:  $P = \mathcal{P}_{>\chi^2}^B \mathcal{P}_{>\chi^2}^F [1 - \ln(\mathcal{P}_{>\chi^2}^B \mathcal{P}_{>\chi^2}^F)]$ . This overall statistical test proves that the  $\Lambda$ CDM-B0 ( $P = 0.14$ ) and  $\Lambda$ CDM2-B2 ( $P = 0.1$ ) models fit well the observational data at a relatively high significance level.

We should conclude that the behaviour of the observed angular correlation function of the X-ray sources is sensitive to the different cosmologies but at the same time there is a strong dependence on the bias models that we have considered in our analysis. By separating between low and high redshift regimes, we obtain results being consistent with the hierarchical clustering scenario, in which the AGN's are strongly biased at all cosmic epochs [10].

## 5. Conclusions

We have studied the clustering properties of the X-ray sources using the predicted angular correlation function for several cosmological



models. We parametrize the predictions for  $w(\theta)$  taking into account the behaviour of  $b(z)$  for a non-bias model, a galaxy conserving bias model with  $b(z) \propto (1+z)$  and for a galaxy merging bias model with  $b(z) \propto (1+z)^{1.8}$ . Utilising the measured angular correlation function, for faint and bright X-ray *ROSAT* sources, estimated in [20] and [1] respectively, we have compared them with the corresponding ones predicted in three cosmological models, namely the  $\tau$ CDM,  $\Lambda$ CDM and  $\Lambda$ CDM2 (with a high  $\sigma_8^{\text{mass}}$  value). We find that the models that best reproduce the observational results are: (1)  $\Lambda$ CDM2 model ( $\Omega_\Lambda = 1 - \Omega_o = 0.7$ ) with high  $\sigma_8^{\text{mass}} = 1.13$  and bias evolution described by  $b(z) \propto (1+z)^{1.8}$  and (2)  $\Lambda$ CDM model ( $\Omega_\Lambda = 1 - \Omega_o = 0.7$ ) with low  $\sigma_8^{\text{mass}} = 0.9$  and bias evolution by  $b(z) \equiv 1$ .

## References

- [1] Akylas, A., Georgantopoulos, I., Plionis, M., 2000, MNRAS, 318, 1036
- [2] Bardeen, J.M., Bond, J.R., Kaiser, N. & Szalay, A.S., 1986, ApJ, 304, 15
- [3] Basilakos S., 2001, MNRAS, *in press*, astro-ph/0104454
- [4] Boyle, B. J., Griffiths, R. E., Shanks, T., Stewart, G. C., Georgantopoulos, I., 1993, MNRAS, 260, 49
- [5] Carrera, F. J., Barcons, X., Fabian, A. C., Hasinger, G., Mason, K. O., McMahon, R. G., Mittaz, J. P. D., Page, M. J., 1998, MNRAS, 299, 229
- [6] Cole, S., Hatton, S., Weinberg, D. H., Frenk, C. S., 1998, MNRAS, 300, 945
- [7] Eke, V., Cole, S., Frenk, C. S., 1996, MNRAS, 282, 263
- [8] Kaiser, N., 1984, ApJ, 284, L9
- [9] Maddox, S., Efstathiou, G., Sutherland, W. J., Loveday, J., 1990, MNRAS, 242, 457
- [10] Magliocchetti, M., Maddox, S. J., Lahav, O., Wall, J. V., 1999, MNRAS, 306, 943
- [11] Martini, P., & Weinberg, D. H., 2000, ApJ, 547, 12
- [12] Matarrese, S., Coles, P., Lucchin, F., Moscardini, L., 1997, MNRAS, 286, 115
- [13] Mo, H.J., & White, S.D.M 1996, MNRAS, 282, 347
- [14] Peebles P.J.E., 1993, Principles of Physical Cosmology, Princeton University Press, Princeton New Jersey
- [15] Perlmutter, S., et al., 1999, ApJ, 517, 565
- [16] Shanks, T., & Boyle, B. J., 1994, MNRAS, 271, 753
- [17] Steidel, C.C., Adelberger, L.K., Dickinson, M., Giavalisko, M., Pettini, M., Kellogg, M., 1998, ApJ, 492, 428
- [18] Sugiyama, N., 1995, ApJS, 100, 281
- [19] Tegmark, M. & Peebles, P.J.E, 1998, ApJ, 500, L79
- [20] Vikhlinin, A. & Forman, W., 1995, ApJ, 455, 109